

# MicroRNA expression profiles from HEK293 cells expressing H5N1 avian influenza virus non-structural protein 1

Innate Immunity  
2019, Vol. 25(2) 110–117  
© The Author(s) 2019  
Article reuse guidelines:  
sagepub.com/journals-permissions  
DOI: 10.1177/1753425919826342  
journals.sagepub.com/home/ini  


Hanwei Jiao , Zonglin Zheng, Xuehong Shuai, Li Wu, Jixuan Chen, Yichen Luo, Yu Zhao, Hongjun Wang and Qingzhou Huang

## Abstract

H5N1 avian influenza poses a serious threat to the poultry industry and human health. Non-structural protein 1 (NS1) plays an important role in the replication and pathogenesis of avian influenza virus (AIV). However, the function of the NS1 gene is still unclear. In this study, illumina genome analyzer iix screening was used to identify the differentially expressed microRNAs (miRNAs) in HEK293 cells expressing H5N1 AIV NS1. There were 13 differentially expressed miRNAs (hsa-miR-17-5p, hsa-miR-221-3p, hsa-miR-22-3p, hsa-miR-31-5p, hsa-miR-20a-5p, hsa-miR-222-3p, hsa-miR-24-3p, hsa-miR-3613-3p, hsa-miR-3178, hsa-miR-4505, hsa-miR-345-3p, hsa-miR-3648, and hsa-miR-455-3p) ( $P < 0.01$ ). The qRT-PCR validation results demonstrated that hsa-miR-221-3p, hsa-miR-22-3p, hsa-miR-20a-5p, and hsa-miR-3613-3p were upregulated, while hsa-miR-3178 and hsa-miR-4505 were down-regulated. The softwares targetscan and miranda were further used to predict their target genes, and the gene ontology (GO) and Kyoto Encyclopedia of Genes and Genomes (KEGG) analysis results showed that 20 GO terms and 20 KEGG pathways were significantly enriched. Our findings are the first to report expression profiling of miRNA and their functions in H5N1 AIV NS1-expressing HEK293 cells, and pave the way to further elucidating the accurate interaction mechanism between NS1 and virus replication, thus providing brand new insight into the prophylaxis and treatment of H5N1 AIV.

## Keywords

H5N1 AIV, NS1, HEK293, miRNAs, target genes

Date Received: 12 August 2018; revised: 28 December 2018; accepted: 5 January 2019

## Introduction

H5N1 is a subtype of avian influenza (AI). The zoonosis caused by H5N1 avian influenza virus (AIV) has attracted much attention worldwide because it is zoonotic and highly pathogenic. AIV has a special mechanism of infecting mammalian cells; it was reported that AIV virulence is related directly to the avian innate immune system.<sup>1–3</sup>

Non-structural protein 1 (NS1) is found mainly in the nucleus and is synthesized largely in the early stages of AIV infection. NS1 can inhibit the production of IFN in infected cells and plays an important role in the antiviral effect of AIV on IFN.<sup>4</sup> NS1 is an important regulator in the process of replication and infection of AIV. The latest research has shown that NS1 can interact with annexin A2 (ANXA2) to modulate

replication of H5N1 AIV.<sup>5</sup> NS1 protein can induce cellular apoptosis via activating reactive oxygen species (ROS) accumulation and mitochondria-mediated apoptotic signaling in chicken oviduct epithelial cells (COECs).<sup>6,7</sup> These reports have shown that the molecular mechanisms linking NS1 and host are very complex.

College of Animal Science, Southwest University, Veterinary Scientific Engineering Research Center, Chongqing, People's Republic of China

### Corresponding author:

Hanwei Jiao, College of Animal Science, Southwest University, Veterinary Scientific Engineering Research Center, Chongqing 402460, People's Republic of China.  
Email: jiaohanwei@swu.edu.cn



MicroRNA (miRNA) is a class of non-coded single-stranded RNA molecules of about 22 nucleotides encoded by endogenous genes, and are involved in the regulation of post-transcriptional gene expression in animals.<sup>8–11</sup> Administration of miR-2911 or a honeysuckle (HS) decoction dramatically reduced mouse mortality caused by H5N1 infection. These results suggested that miR-2911 is involved directly in the process of H5N1 AIV infection.<sup>12</sup> Since recent research has shown that gga-miR-1644 targets muscle blind-like protein 2 (MBNL2), and gga-miR-6675 targets polymerase basic protein 1 (PB1) to regulate the ability of the H9N2 AIV replication, this study may provide brand new insights into the interaction of avian miRNAs with avian DCs and the inhibition of virus replication.<sup>13</sup>

Here, we aimed to reveal the interaction between NS1 and miRNAs in host cells. We reconstructed stable NS1-EGFP and EGFP cell lines. miRNA-Seq-based screening was performed to identify the differential expression miRNA profiling in NS1-expressing HEK293 cells, qRT-PCR was used to validate them, their target genes were predicted by targetscan and miranda software, and the confirmed miRNAs were assigned functions by gene ontology (GO) and Kyoto Encyclopedia of Genes and Genomes (KEGG) analysis.

## Materials and methods

### Construction of NS1-expressing HEK293 cells

The HEK293 cell line was purchased from the Cell Bank of the Chinese Academy of Science (Shanghai, China) and cultured at 5% CO<sub>2</sub>, 37°C, in DMEM (Thermo Scientific, San Diego, CA) containing 10% heat-inactivated FBS (Thermo Scientific), supplemented with penicillin (100 U/ml) (Thermo Scientific) and streptomycin (100 µg/ml) (Thermo Scientific). Recombinant plasmids pEGFP-N1 and pNS1-EGFP, which express H5N1 AIV NS1-EGFP fusion protein, were transfected into HEK293 cells with lipofectamine<sup>TM</sup> 3000, and NS1-EGFP and EGFP stable cell lines were constructed, as identified by fluorescence microscopy (Olympus, Tokyo, Japan) observation. FACSCalibur flow cytometer (Becton-Dickinson, Franklin Lakes, NJ) determination and Western blotting detection were performed according to our previous research.<sup>14</sup>

### miRNA array screening

Small RNAs were extracted from the NS1-EGFP and EGFP stable cell lines, named NS and E, respectively. Of each group, three independent samples were

prepared; a total of six samples were chosen randomly for an initial genome-wide microarray screening. An mParaflo miRNA microarray assay was performed by an external service provider, as previously described.<sup>15</sup> miRNAs that were significantly differentially expressed ( $P < 0.01$ ) based on the miRNA array were selected for further qRT-PCR validation and functional enrichment analysis.

### qRT-PCR validation for miRNA profiling

miRNA profiling was verified using an miRNA specific-TaqMan<sup>®</sup> probe (Thermo Scientific), and qRT-PCR was used to validate the differentially expressed miRNAs ( $P < 0.01$ ). U6 snRNA (Thermo Scientific) was used as an internal control. Three independent repeated experiments were performed as described previously.<sup>16</sup>

### Prediction of target genes of the confirmed miRNAs

Two online target prediction software programs, targetscan and miranda, were used to predict target genes of miRNAs ( $P < 0.01$ ). The prediction results were screened according to the grading criteria of each software. Finally, the data predicted by both softwares were combined and overlaps were calculated.

### GO and KEGG functional enrichment analysis of miRNAs

According to our previous study, GO and KEGG were performed to analyze the miRNAs.<sup>15</sup> GO annotations were divided into biological process, cellular components, and molecular function categories; each term corresponds to one category. Pathway analysis helps further understand the biological functions of genes. KEGG is the major public database of pathways; pathways were analyzed by significance enrichment. Using the KEGG pathway as a unit, we applied hypergeometric testing to find out the background of the whole genome. Pathways were significantly enriched in significant differentially expressed genes (DEGs).

### Statistical analysis

Data were analyzed with the Student's *t*-test and one-way ANOVA.  $P < 0.05$  was considered statistically significant, and  $P < 0.01$  was considered statistically highly significant.

## Results

### miRNA profilings in NS1-expressing HEK293 cells

NS1-EGFP and EGFP stable cell lines were constructed according to our previous research,<sup>14</sup> and expression of EGFP and NS1-EGFP fusion protein were detected by fluorescence microscopy and Western blotting. The percentage of positive rate and the fluorescent mean

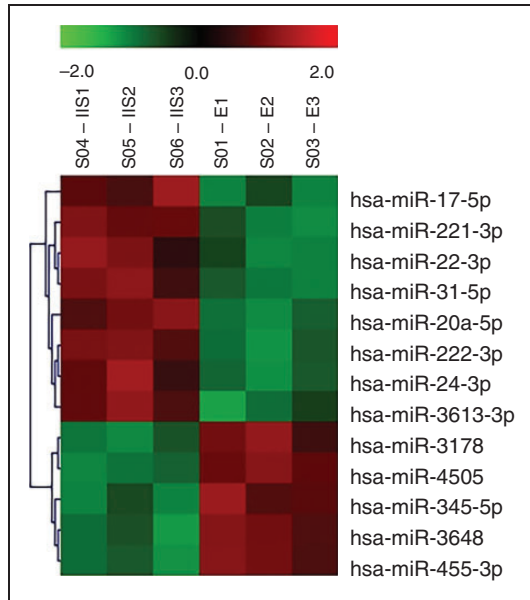


**Figure 1.** Heatmap of differentially expressed miRNAs in NS1-expressing HEK293 cells ( $P < 0.01$ ). NS, NS1-EGFP stable cell line; E EGFP stable cell line. NS-1, NS-2, and NS-3 represent the samples of three independently repeated experiments, respectively, as do E1, E2 and E3. The red color part represents upregulated expression, and green color, down-regulated expression.

value of the stable cells lines were detected by flow cytometry, as shown in Supplementary Figure 1.

The small RNAs of NS and E were extracted from the NS1-EGFP and EGFP stable cell lines. High-throughput based microarray screening was performed. As shown in Figure 1, there were 3 differentially expressed miRNAs ( $P < 0.01$ ), namely hsa-miR-17-5p, hsa-miR-221-3p, hsa-miR-22-3p, hsa-miR-31-5p, hsa-miR-20a-5p, hsa-miR-222-3p, hsa-miR-24-3p, hsa-miR-3613-3p, hsa-miR-3178, hsa-miR-4505, hsa-miR-345-3p, hsa-miR-3648, and hsa-miR-455-3p. The  $P$  values, group E means, group NS means and  $\log_2$  (NS/E) values of these are shown in Table 1.

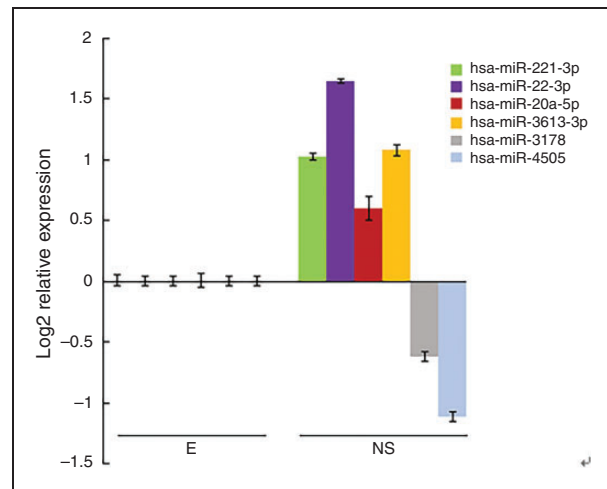


**Figure 2.** qRT-PCR validation of differentially expressed miRNA profiling obtained from the miRNA microarray assay. Up-regulation of hsa-miR-221-3p, hsa-miR-22-3p, hsa-miR-20a-5p, and hsa-miR-3613-3p was confirmed, as well as down-regulation of hsa-miR-3178 and hsa-miR-4505.

**Table 1.** The significantly differentially expressed miRNAs identified by microarray analysis.

| Reporter name   | P-Value  | Group1<br>E<br>Mean | Group2<br>NS<br>Mean | Log <sub>2</sub> (G2/G1) |
|-----------------|----------|---------------------|----------------------|--------------------------|
| hsa-miR-17-5p   | 6.08E-03 | 3,034               | 4,955                | 0.71                     |
| hsa-miR-221-3p  | 7.94E-03 | 1,654               | 3,421                | 1.05                     |
| hsa-miR-22-3p   | 9.68E-03 | 184                 | 594                  | 1.69                     |
| hsa-miR-31-5p   | 2.61E-03 | 418                 | 655                  | 0.65                     |
| hsa-miR-20a-5p  | 1.39E-03 | 3,106               | 4,606                | 0.57                     |
| hsa-miR-222-3p  | 2.11E-03 | 2,625               | 5,065                | 0.95                     |
| hsa-miR-24-3p   | 6.86E-03 | 756                 | 1,016                | 0.43                     |
| hsa-miR-3613-3p | 7.19E-03 | 598                 | 1233                 | 1.04                     |
| hsa-miR-3178    | 4.05E-03 | 11,642              | 7,211                | -0.69                    |
| hsa-miR-4505    | 7.43E-03 | 1,124               | 509                  | -1.14                    |
| hsa-miR-345-3p  | 4.72E-03 | 55                  | 30                   | -0.86                    |
| hsa-miR-3648    | 3.03E-03 | 76                  | 19                   | -1.98                    |
| hsa-miR-455-3p  | 2.07E-03 | 174                 | 76                   | -1.19                    |

### qRT-PCR validation of the 13 differentially expressed miRNAs

To validate the miRNA profiling, miRNA specific TaqMan® probes of the 13 differentially expressed miRNAs were obtained, and qRT-PCR was performed to confirm the miRNA array-based data. U6 snRNA was used as an internal control. As shown in Figure 2, when compared with the E group, the qRT-PCR validation results showed that hsa-miR-221-3p, hsa-miR-22-3p, hsa-miR-20a-5p, and hsa-miR-3613-3p were upregulated, and hsa-miR-3178 and hsa-miR-4505 were down-regulated in NS1-expressing HEK293 cells. The qRT-PCR validation  $\Delta\Delta C_T$  values of the E and NS groups are shown in Table 2.

**Table 2.** The qRT-PCR validation  $\Delta\Delta C_T$  value of the E and NS groups.

| Reporter name   | $\Delta\Delta C_T$ |               |
|-----------------|--------------------|---------------|
|                 | Group I<br>E       | Group 2<br>NS |
| hsa-miR-221-3p  | 0                  | 1.02          |
| hsa-miR-22-3p   | 0                  | 1.65          |
| hsa-miR-20a-5p  | 0                  | 0.60          |
| hsa-miR-3613-3p | 0                  | 1.08          |
| hsa-miR-3178    | 0                  | -0.62         |
| hsa-miR-4505    | 0                  | -1.11         |

### Prediction of target genes of the six differentially expressed miRNAs and GO functional enrichment analysis

The targetscan and miranda software programs were used to predict the target genes of the six differentially expressed miRNAs. In the targetscan algorithm, target genes with a context score percentile of < 50 were removed. In the miranda algorithm, target genes with maximum free energy (Max Energy) greater than -10 were removed. Finally, the overlap of the two software programs was taken to represent the final target genes of the six differentially expressed miRNAs.

As shown in Figure 3, the target genes of the six confirmed miRNAs were assigned to three categories: biological process, cellular component, and molecular function ( $P < 0.05$ ), and the percentage of the genes of 50 GO terms were determined (Supplementary Table S1).

Further, a functional enrichment analysis of all GO terms was performed. As shown in Figure 4, 20 GO terms were significantly enriched, and the target genes of these are shown in Supplementary Table S2. The enrichment factor indicated the number of differential genes located in the GO relative to the total GO base, and the smaller the  $P$  value, the higher the concentration of GO.

### Prediction of target genes of the six differentially expressed miRNAs and KEGG functional enrichment analysis

Target genes were predicted as above. As shown in Figure 5, functional enrichment analysis of the

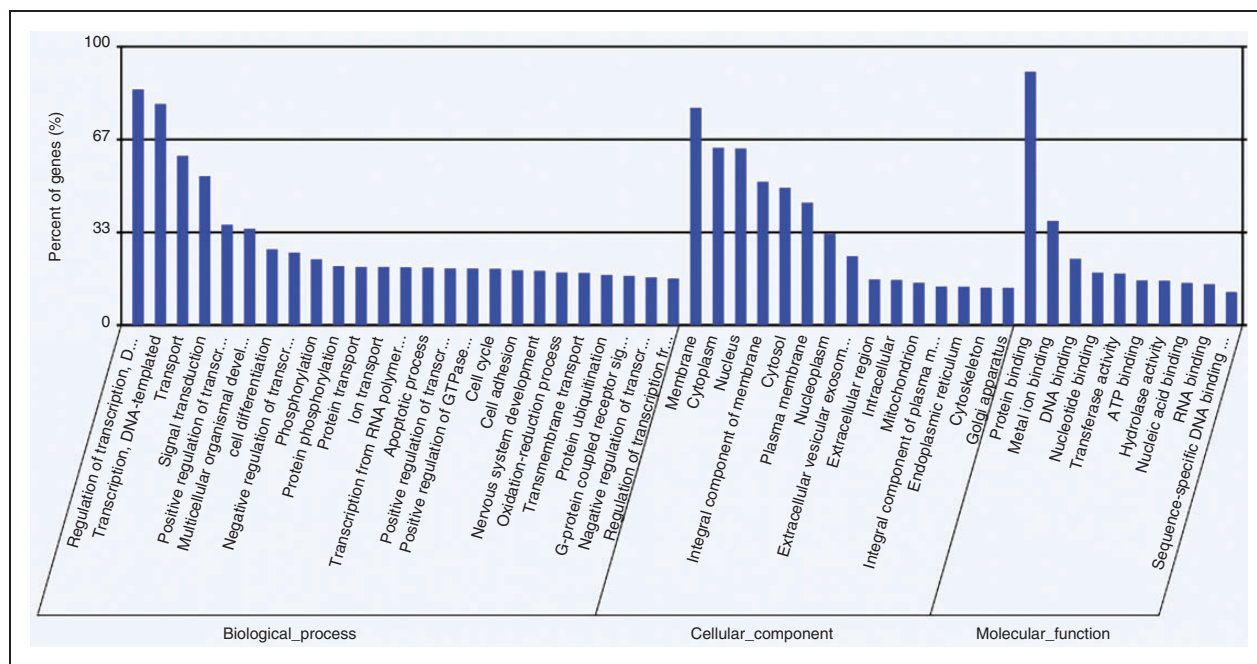


**Figure 3.** GO classifications for the predicted target genes of the six differentially expressed miRNAs.

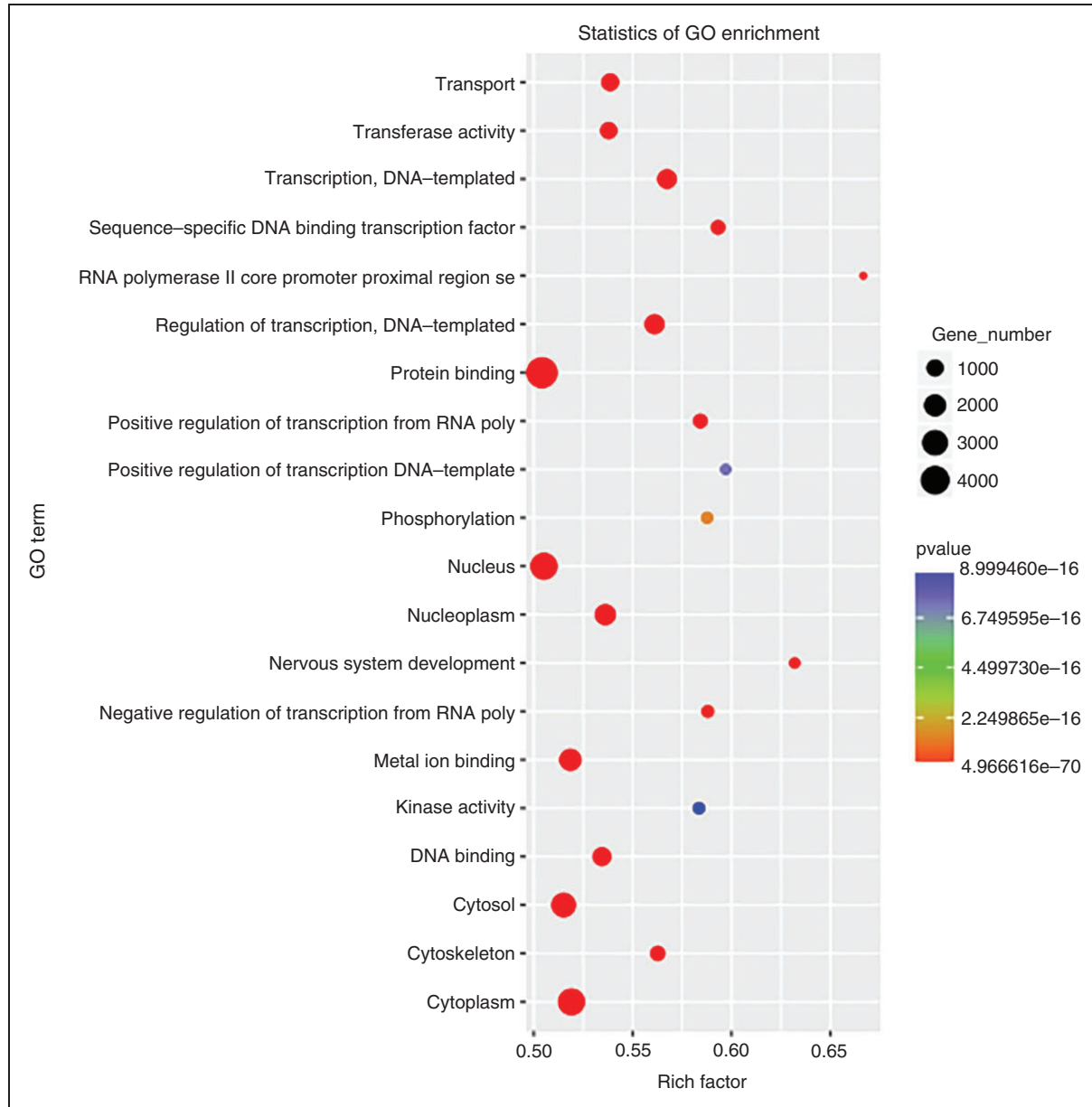


**Figure 4.** GO functional enrichment analysis of the predicted target genes of the six differentially expressed miRNAs. y-axis: GO terms; x-axis: rich factor. The color of each bubble represents the *P* value, and bubble size the gene number.

pathway was performed. Twenty KEGG pathways were significantly enriched, the target genes of which are shown in Supplementary Table S3. The enrichment factor indicated the number of differential genes located in the KEGG relative to the total base of the KEGG, and, the smaller the *P* value, the higher the concentration of KEGG.

## Discussion

H5N1 is the most common AIV and represents an important pathogen for zoonosis. New vaccines against

highly pathogenic AIV have been strongly discussed worldwide.<sup>17–20</sup> In the process of AIV infection in birds, NS1 proteins mediate the translation and replication of viral proteins by affecting host signaling pathways. There were reports that the poly ADP-ribose polymerase 10 (PARP10) protein was synergistic with H5N1 subtype AIV NS1 protein and co-regulated the replication process of AIV virus.<sup>21</sup>

Genome microarray experiments were used to identify the DEGs in chicken embryo fibroblasts (CEF) stimulated by the highly pathogenic H5N1 AIV, providing new insights into how AIV affects expression of

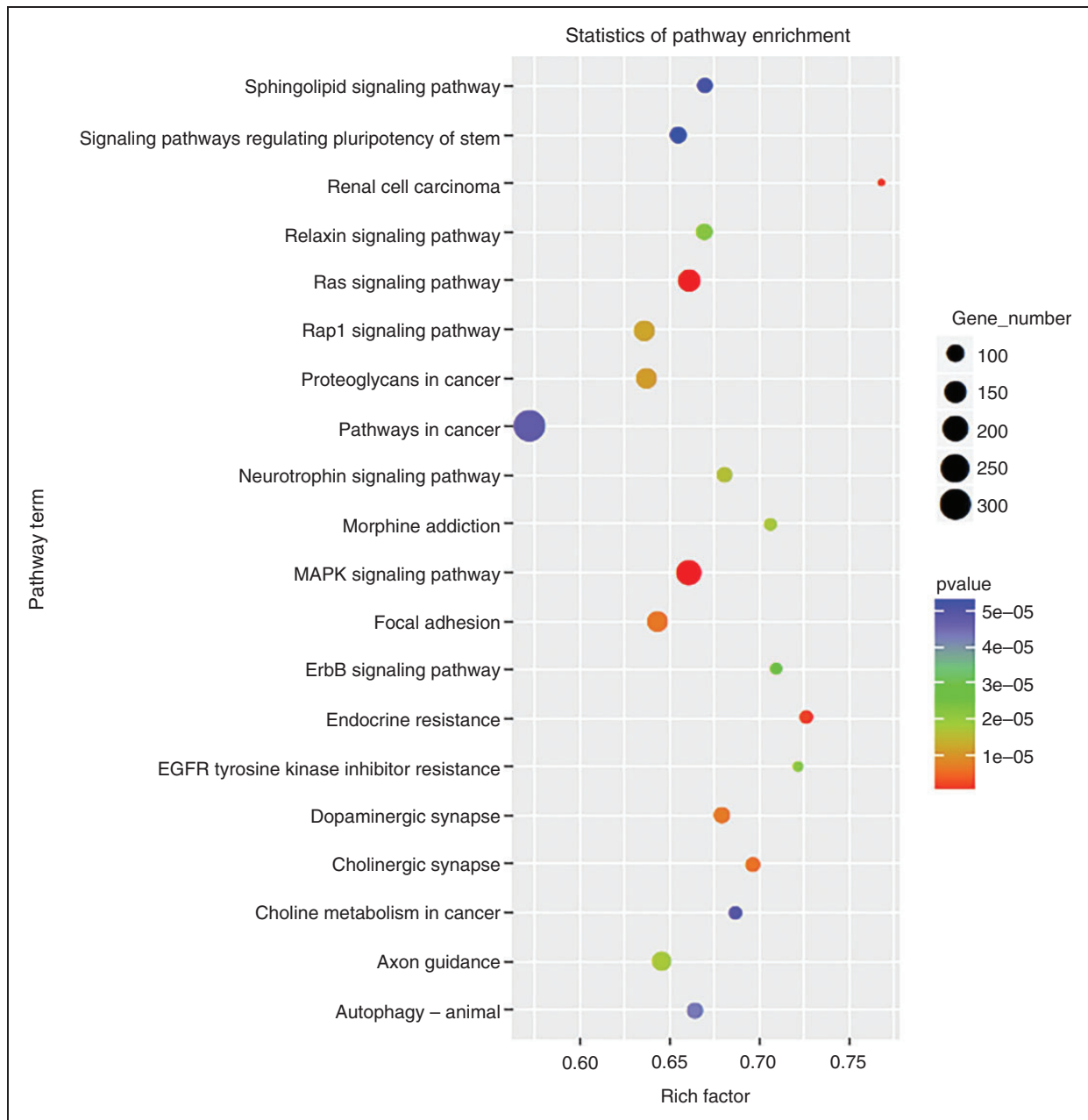


**Figure 5.** KEGG functional enrichment analysis of the predicted target genes of the six differentially expressed miRNAs. y-axis: pathway terms; x-axis: rich factor. The color of each bubble represents the P value and bubble size the gene number.

host genes, as well as the host immune response and viral replication.<sup>22</sup> Our study was performed to reveal the molecular mechanism of AIV-infected HEK293 target cells, and to identify how the differentially expressed miRNAs affect the host response and replicate in host cells. Stable E and NS cell lines were constructed, and small RNAs extracted. An initial genome-wide microarray screening was performed to identify the miRNA profiling, and qRT-PCR validation results showed that there were six differentially expressed miRNAs, consistent with the results of the

array-based chip. However, there were seven false positive miRNAs that could not be validated by qRT-PCR. The reason for this might be that the transcripts were statistically significant but had low signals (< 500) and the mean values were too low to confirm.

The hsa-miR-221-3p plays an important role in the diagnosis of breast cancer (BC) and other tumors. The interaction between hsa-miRNA-221-3p and its target gene may serve as a molecular marker for the diagnosis of BC, and as a target for subsequent treatment.<sup>23</sup> Long non-coding RNAs (lncRNAs) play an important

role in many cancers and tumor pathogenesis, e.g., lncRNA digeorge syndrome critical region gene 5 (DGCR5) inhibits expression of hsa-miR-22-3p, which promotes the development of lung adenocarcinoma (LUAD).<sup>24</sup> LncRNAs and hsa-miR-20a-5p co-target the target gene transcription 1, which mediates hepatocellular carcinoma (HCC) growth, cell cycle progression, and the migration process.<sup>25</sup> In HCC, hsa-miR-3613-3p affects cell proliferation and the cell cycle, and is considered as a biomarker and therapeutic target for liver cancer.<sup>26</sup> The hsa-miRNA-3178 regulates expression of the target gene early growth responsive gene 3 (EGR3), thereby mediating the proliferation, invasion, angiogenesis and apoptosis of HCC tumor endothelial cells (TECs).<sup>27</sup> No research on hsa-miR-4505 has been reported yet.

miRNA microarray chip analysis was performed to investigate the functions of H5N1 AIV NS1. Each sample of total RNA first passed quality control, and the whole chip experiment process, included labeling, chip hybridization, hybridization signal amplification, and image acquisition, was then carried out. Six miRNAs were identified in the array-based screen. Up-regulation of hsa-miR-221-3p, hsa-miR-22-3p, hsa-miR-20a-5p, and hsa-miR-3613-3p, and down-regulation of hsa-miR-3178 and hsa-miR-4505 were validated, mediated by a stable expression of H5N1 AIV NS1 protein in HEK293 cells. Bioinformatic software tools were used to predict the target genes of the six confirmed miRNAs and to determine their functional enrichment. Transfection of miRNA mimics, miRNA inhibitors and 3'UTR dual-luciferase reporter gene experiments will be performed further to identify the target genes of the six miRNAs, which may help elucidate the regulatory relationship between H5N1 AIV NS1 and the host.

This study is the first to report expression profiling of miRNAs and determining their functions in HEK293 cells stably expressing NS1 protein of H5N1 AIV. However, future research should focus not only on how to elucidate the accurate interaction mechanism between NS1 and virus replication, but also on how to reveal NS1 affecting the host immune response. Our findings provide new insights into possible routes for the prophylaxis and treatment of H5N1 AIV.

#### Declaration of conflicting interests

The author(s) declared no potential conflicts of interest with respect to the research, authorship, and/or publication of this article.

#### Funding

The author(s) disclosed receipt of the following financial support for the research, authorship, and/or publication of this

article: This study was supported financially by the National Science Foundation for Young Scientists of China (No. 31802215), the Natural Science Foundation of Chongqing (Chongqing Research Program of Basic Research and Frontier Technology: No. cstc2018jcyjA0807), and the Research Funding project of Southwest University (No. 20700505).

#### ORCID iD

Hanwei Jiao  <http://orcid.org/0000-0001-8001-8697>

#### References

1. Liniger M, Moulin HR, Sakoda Y, et al. Highly pathogenic avian influenza virus H5N1 controls type I IFN induction in chicken macrophage HD-11 cells: a polygenic trait that involves NS1 and the polymerase complex. *Virology* 2012; 9: 7–18.
2. Park S, Choi J, Jeun M, et al. Detection of avian influenza virus from cloacal swabs using a disposable Well Gate FET sensor. *Adv Healthc Mater* 2017; 6: 1700371–1700376.
3. Jiang W, Hou G, Li J, et al. Novel variants of clade 2.3.2.1 H5N1 highly pathogenic avian influenza virus in migratory waterfowl of Hongze Lake. *Vet Microbiol* 2017; 198: 99–103.
4. Xing Z, Cardona CJ, Adams S, et al. Differential regulation of antiviral and proinflammatory cytokines and suppression of Fas-mediated apoptosis by NS1 of H9N2 avian influenza virus in chicken macrophages. *J Gen Virol* 2009; 90: 1109–1118.
5. Ma Y, Sun J, Gu L, et al. Annexin A2 (ANXA2) interacts with nonstructural protein 1 and promotes the replication of highly pathogenic H5N1 avian influenza virus. *BMC Microbiol* 2017; 17: 191–199.
6. Qi X, Zhang H1, Wang Q, et al. The NS1 protein of avian influenza virus H9N2 induces oxidative-stress-mediated chicken oviduct epithelial cells apoptosis. *J Gen Virol* 2016; 97: 3183–3192.
7. Wu H, Peng X, Peng X, et al. Amino acid substitutions involved in the adaptation of a novel highly pathogenic H5N2 avian influenza virus in mice. *Virology* 2016; 13: 159–163.
8. Nguyen TH, Liu X, Su ZZ, et al. Potential role of MicroRNAs in the regulation of antiviral responses to influenza infection. *Front Immunol* 2018; 9: 1541–1553.
9. To KK, Tong CW, Wu M, et al. MicroRNAs in the prognosis and therapy of colorectal cancer: From bench to bedside. *World J Gastroenterol* 2018; 24: 2949–2973.
10. Monsanto-Hearne V, Johnson KN. miRNAs in insects infected by animal and plant viruses. *Viruses* 2018; 10: 354–362.
11. Pong SK and Gullerova M. Non-canonical functions of microRNA pathway enzymes—Drosha, DGCR8, Dicer and Ago proteins. *FEBS Lett* 2018; 592: 2973–2986.
12. Zhou Z, Li X, Liu J, et al. Honeysuckle-encoded atypical microRNA2911 directly targets influenza A viruses. *Cell Res* 2015; 25: 39–49.

13. Lin J, Xia J, Zhang T, et al. Genome-wide profiling of microRNAs reveals novel insights into the interactions between H9N2 avian influenza virus and avian dendritic cells. *Oncogene* 2018; 37: 4562–4580.
14. Jiao H, Du L, Hao Y, et al. Effective inhibition of mRNA accumulation and protein expression of H5N1 avian influenza virus NS1 gene in vitro by small interfering RNAs. *Folia Microbiol* 2013; 58: 335–342.
15. Xu K, Guo S, Zhao T, et al. Transcriptome analysis of HepG2 cells expressing ORF3 from swine hepatitis E virus to determine the effects of ORF3 on host cells. *Biomed Res Int* 2016; 2016: 1648030.
16. Rong H, Jiao H, Hao Y, et al. CD14 gene silencing alters the microRNA expression profile of RAW264.7 cells stimulated by *Brucella melitensis* infection. *Innate Immun* 2017; 23: 424–431.
17. Kim SH and Samal SK. Heterologous prime-boost immunization of Newcastle disease virus vectored vaccines protected broiler chickens against highly pathogenic avian influenza and Newcastle disease viruses. *Vaccine* 2017; 35: 4133–4139.
18. Tabynov K, Sansyrbay A, Sandybayev N, et al. The pathogenicity of swan derived H5N1 virus in birds and mammals and its gene analysis. *Virol J* 2014; 11: 207.
19. Yu Y, Zhang Z, Li H, et al. Biological characterizations of H5Nx avian influenza viruses embodying different neuraminidases. *Front Microbiol* 2017; 8: 1084–1093.
20. Hassan MM, Hoque MA, Debnath NC, et al. Are poultry or wild birds the main reservoirs for avian influenza in Bangladesh? *Ecohealth* 2017; 14: 490–500.
21. Yu M, Zhang C, Yang Y, et al. The interaction between the PARP10 protein and the NS1 protein of H5N1 AIV and its effect on virus replication. *Virol J* 2011; 8: 546–555.
22. Sarmento L, Afonso CL, Estevez C, et al. Differential host gene expression in cells infected with highly pathogenic H5N1 avian influenza viruses. *Vet Immunol Immunopathol* 2008; 125: 291–302.
23. Abak A, Amini S, Estiar MA, et al. Analysis of miRNA-221 expression level in tumors and marginal biopsies from patients with breast cancer (cross-sectional observational study). *Clin Lab* 2018; 64: 169–175.
24. Dong HX, Wang R, Jin XY, et al. LncRNA DGCR5 promotes lung adenocarcinoma (LUAD) progression via inhibiting hsa-mir-22-3p. *J Cell Physiol* 2018; 233: 4126–4136.
25. Cao MR, Han ZP, Liu JM, et al. Bioinformatic analysis and prediction of the function and regulatory network of long non-coding RNAs in hepatocellular carcinoma. *Oncol Lett* 2018; 15: 7783–7793.
26. Zhang D, Liu E, Kang J, et al. MiR-3613-3p affects cell proliferation and cell cycle in hepatocellular carcinoma. *Oncotarget* 2017; 8: 93014–93028.
27. Li W, Shen S, Wu S, et al. Regulation of tumorigenesis and metastasis of hepatocellular carcinoma tumor endothelial cells by microRNA-3178 and underlying mechanism. *Biochem Biophys Res Commun* 2015; 464: 881–887.